ISSN 1330-3651 (Print), ISSN 1848-6339 (Online)
DOI: 10.17559/TV-20140211130812

SEM/EDX, XPS, CORROSION AND SURFACE ROUGHNESS CHARACTERIZATION OF AISI 316L SS AFTER ELECTROCHEMICAL TREATMENT IN CONCENTRATED HNO_3

Krzysztof Rokosz, Tadeusz Hryniewicz, Steinar Raaen, Jan Valiček

Original scientific paper

In the paper there is described the AISI 316L stainless steel surface obtained after electrochemical treatment in concentrated HNO_3. It was characterized by roughness parameters, corrosion protection behaviour and chemical composition of the surface layer. Generally used 2D and 3D roughness parameters describing the surface after the electrochemical treatment are the following: Ra = 0.737 μm and Sa = 1,13 μm as well as Rq = 0,895 μm and Sq = 1,37 μm. In case of corrosion studies the passive current density was equal to $2{,}3\times10^{-2}$ μA/cm^2, pitting potential was equal to E_{pit} = 1140 mV vs. SCE and re-passivation potential was 79 mV vs. SCE. In the surface layer there were detected compounds of iron, chromium, molybdenum, cobalt, manganese, as well as calcium (contamination). The high resolution XPS spectra/results data have shown that most of detected iron compounds can be described as Fe_2O_3/FeOOH and chromium compounds as Cr_2O_3/CrOOH. The molybdenum detected in the surface layer was mainly in valency states six (65 at%) and five (17 at%).

Keywords: *AISI 316L SS; corrosion characteristics; electrochemical treatment; HNO_3; surface roughness; XPS*

SEM/EDX, XPS, korozija i karakterizacija hrapavosti površine AISI 316L SS nakon elektrokemijske obrade u koncentriranoj HNO_3

Izvorni znanstveni članak

U radu se opisuje površina nehrđajućeg čelika AISI 316L poslije elektrokemijske obrade u koncentriranoj HNO_3. Obilježena je prametrima hrapavosti, ponašanjem kod zaštite od korozije i kemijskim sastavom površinskog sloja. Uobičajeno korišteni 2D i 3D parametri hrapavosti koji opisuju površinu nakon elektrokemijske obrade su sljedeći: Ra = 0,737 μm i Sa = 1,13 μm kao i Rq = 0,895 μm i Sq = 1,37 μm. Kod proučavanja korozije pasivna gustoća struje bila je $2{,}3\times10^{-2}$ μA/cm^{2,} potencijal točkaste korozije E_{pit} = 1140 mV vs. SCE i mogućnost ponovnog pasiviziranja bio je 79 mV vs. SCE. U površinskom su sloju otkriveni spojevi željeza, kroma, molibdena, kobalta, mangana, kao i kalcija (zagađenost). Rezultati visoke rezolucije XPC spektra pokazali su da se većina pronađenih željeznih spojeva može opisati kao Fe_2O_3/FeOOH, a spojevi kroma kao Cr_2O_3/CrOOH. Molibden otkriven u površinskom sloju bio je uglavnom sa strukturom valencija šest (65 at%) i pet (17 at%).

Ključne riječi: *AISI 316L SS; elektrokemijska obrada; HNO_3; XPS; značajke korozije; hrapavost površine*

1 Introduction

Stainless steels are commonly treated by electropolishing considered as a standard electrochemical process/treatment [1 ÷ 6]. The process is generally used in industry for finishing operations and is often carried out in the mixture of two acids, H_2SO_4 and H_3PO_4 [7 ÷ 10]. After this process a treated part reveals smooth and bright surface with good corrosion resistance and improved mechanical properties [10 ÷ 16]. It is of special importance when using that stainless steel as a biomaterial. Concerning improved corrosion resistance [12 ÷ 18], the steel parts may be chemically treated in concentrated nitric acid and that process is described in the literature [19 ÷ 21]. On the other hand, there are no study results available on electrochemical treatment of stainless steels in concentrated nitrogen acid.

The use of an oxidizing acid, such as nitric acid, for passivation has two purposes. First of all, the acid dissolves any surface inclusions in the steel. Secondly, it assures a uniform, clean surface those results in the consistent formation of the passive chromium oxide film (and molybdenum film) [2]. The passivation process enhances the chromium fraction in the passive film, as established before [4, 12, 16]. The main mechanism for this process is selective dissolution of predominantly iron [3, 4]. In addition to the chemical process with a standard immersion in nitric acid solution the electrochemical treatment is proposed.

The aim of the study is to perform electropolishing of AISI 316L stainless steel in HNO_3 and investigate the surface properties after that operation. Specifically, the study of the corrosion behaviour of that steel in a typical Ringer's solution [7, 13, 16] was investigated. Thorough characterization of such obtained 316L steel surface may be of a great practical value.

2 Method

2.1 Material

For the study there were used samples of the AISI 316L austenitic chromium-nickel-molybdenum stainless steel. The addition of molybdenum to the stainless steel increases corrosion resistance and mechanical properties. Typically that sort of steel is very often used in food, pharmaceutical, marine, architecture applications, as well as applied for biomaterial. The bulk composition of the steel, by standard, and as-measured, is shown in Tab. 1. Second column of Tab. 1 presents composition provided by the manufacturer [15].

Ten samples of AISI 316L stainless steel as received of dimensions 60×30×1 (mm) were prepared for the studies. They were treated by electrochemical treatment in concentrated HNO_3 under defined conditions, with the current density used i = 65±5 A/dm^2. The electrochemical polishing process was carried out for 3 minutes time in the electrolyte of temperature of 65 °C, with the temperature control of ±10 °C. The electrolytic cell was made of glass, containing up to 500 cm^3 of electrolyte. Afterwards the samples were rinsed in distilled water for about 2 minutes and dried in air for about 3 minutes.

Table 1 Chemical composition of AISI 316L stainless steel

Element	Typical composition, wt%	Content as measured, wt%
Chromium	16 ÷ 18	16,92
Nickel	10 ÷ 14	10,38
Manganese	2 (max)	1,30
Molybdenum	2 ÷ 3	2,01
Nitrogen	0,1 (max)	0,04
Carbon	0,03 (max)	0,02
Silicon	0,75 (max)	0,39
Phosphorus	0,045 (max)	0,32
Sulphur	0,03 (max)	0,01
Copper	-	0,28
Vanadium	-	0,09
Cobalt	-	0,19
Aluminium	-	0,01
Iron	Balance	68,04

The surface roughness studies were carried by interferometric method with Taylor-Hobson Precision Talysurf CCI 6000 (Coherent Correlation Interferometry). The SEM/EDX measurements were performed on ASPEX EXPLORER™ apparatus. The XPS experiments were carried out in an ultra-high-vacuum system with a base pressure of about 10^{-8} Pa. The XPS measurements, with the angle of 90°, were performed using a SES2002 electron energy analyzer with a monochromatized Al Kα ($h\nu$ = 1486,6 eV) X-ray source (Gammadata-Scienta). A total resolution of about 0,6 eV was obtained for the presented spectra. In view of optimizing the signal-to-noise ratio, one XPS measurement cycle covered 100 sweeps. For the XPS analyses the CasaXPS 2.3.14 software was used [22 ÷ 24]. The XPS spectra were analysed by using Shirley background and GL(30), LA(1,2; 4,8; 3), LA(1,3; 4; 5) line shapes [25 ÷ 29].

Corrosion studies after electrochemical treatment were carried out in a typical Ringer's physiological fluid, at 25 °C. The electrochemical system used for the corrosion measurements consisted of a potentiostat ATLAS 98 with the software IMP98, a platinum counter electrode Ept-101, and a saturated calomel reference electrode EK-101P. The corrosion measurements data were recorded every 5 mV with the rate of 0,1 mV/s. In the case of the potentiodynamic measurements the specimens were immersed in the same solution for 1 hour prior to the measurement in order to stabilize the surface at the conditions of open circuit potential.

3 Study results

In Fig. 1 there are shown the SEM photo and EDX spectrum of surface after electrochemical treatment in concentrated HNO_3. The structure of the treated steel surface is revealed and, on the basis of the EDX results one may easily notice there is a possibility to determine the chemical composition of the obtained surface. In that case there were detected the biggest signals from iron, chromium and nickel.

In order to investigate in detail the chemical composition of surface layer formed after electrochemical treatment in concentrated HNO_3, the XPS spectroscopy as survey scan (Fig. 2) was used. On the basis of that method, in surface layer there were more chemical elements than only iron, chromium and nickel detected, with such additional elements like oxygen, molybdenum, cobalt, manganese, as well as calcium as contamination. The survey of XPS study has shown more information about the surface layer than that from EDX, but still not enough. In that situation there were used the high resolution XPS measurements for iron, chromium and molybdenum; they are presented in Figs. 3 ÷ 5 and in Tabs. 2 ÷ 4.

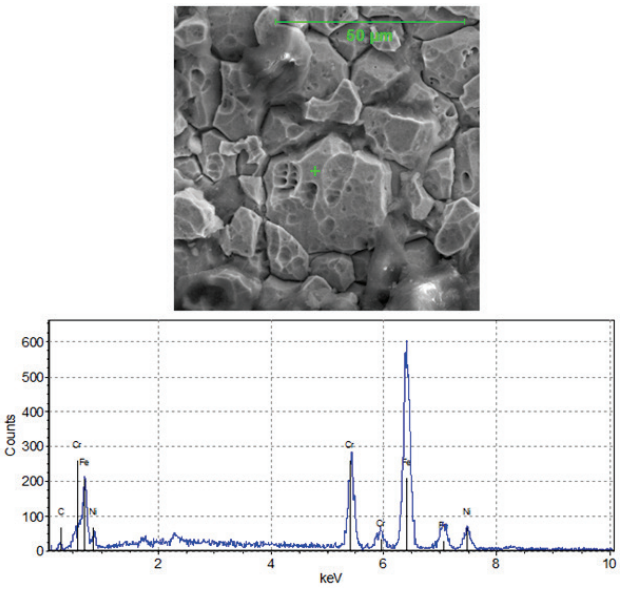

Figure 1 SEM/EDX results of AISI 316L SS after electrochemical treatment in concentrated HNO_3

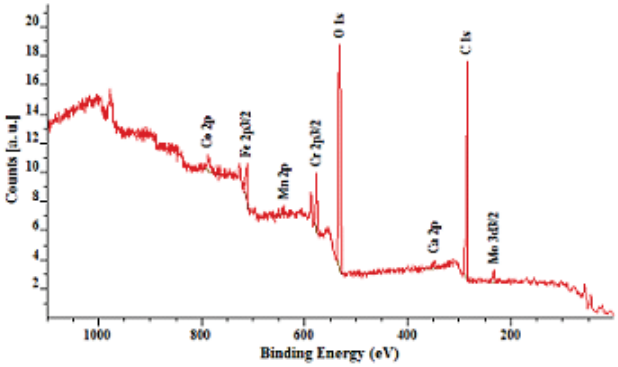

Figure 2 XPS survey results of AISI 316L SS after electrochemical treatment in concentrated HNO_3

The Fe 2p spectrum was fitted by two peaks: one line for iron metal Fe-M and the second one for a compound part Fe-X. Shape lines for iron spectrum fitting from GL(30) (metal and compounds spectrum part) and LA(1.2,4.8,3) (metal part) were selected. On the basis of results shown in Fig. 3 and Tab. 2 it is visible that the atomic percent of iron metal is in the range of 4,3 ÷ 4,4 at% and percent of iron compounds amounts for 95,6 ÷ 95,7 at%.

Fitting by two peaks is not the best method, but with well-chosen line shapes it should provide essential information about the predominance of oxides, hydroxides as well as phosphates and sulphates of iron. Therefore two peaks analysis for binding energy 711,5 eV was performed. In the presented data the most probable chemical iron compound appears to be a mixture of Fe_2O_3/FeOOH.

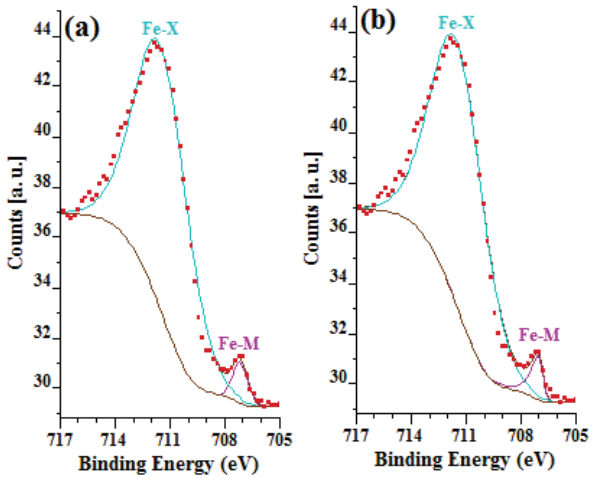

Figure 3 XPS high resolution of Fe 2p3/2 spectra fitting by GL(30) shape lines (a) and LA(1,2; 4,8; 3) plus GL(30) (b); RSTD (Residual Standard Deviation) of two peaks analysis 0,066, analysis by LA(1,2; 4,8; 3) plus GL(30) shape lines; RSTD of two peaks analysis 0,064, analysis by GL(30) shape lines

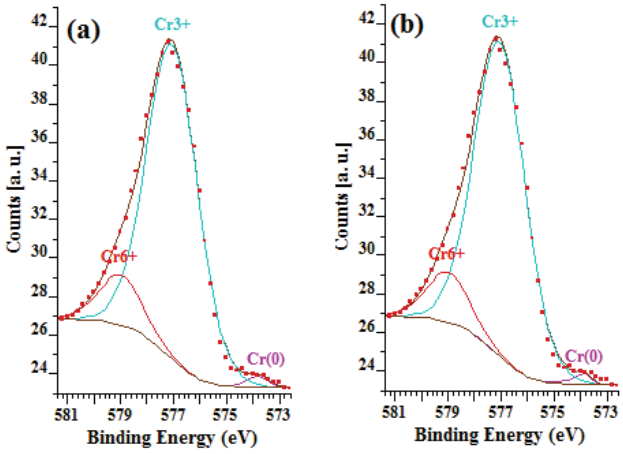

Figure 4 XPS high resolution of Cr $2p_{3/2}$ spectra fitting by GL(30) shape lines (a) and LA(1,3; 4; 5) plus GL(30) (b); RSTD (Residual Standard Deviation) of analyses by LA(1,3; 4; 5) plus GL(30) shape lines is 0,061; RSTD of analysis by GL(30) shape lines is also 0,061

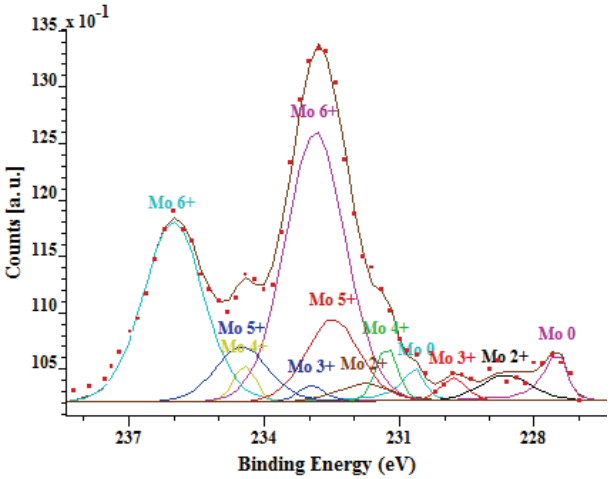

Figure 5 XPS high resolution results of AISI 316L SS after electrochemical treatment in concentrated HNO_3, RSTD=0,034; (RSTD: Residual Standard Deviation)

Table 2 Analyses of Fe 2p spectrum by GL(30) and LA(1,2; 4,8; 3) line shapes

BE / eV	707,1	711,5	707,0	711,5
FWHM	0,970638	3,38146	0,464694	3,36522
Line shape	GL(30)	GL(30)	LA(1,2; 4,8; 3)	GL(30)
AREA	1,7	38,5	1,8	38,4
Fe $2p_{3/2}$ / at%	4,3	95,7	4,4	95,6
Iron compounds	Fe-M	Fe-X	Fe-M	Fe-X

In Fig. 5 and Tab. 4 there are shown the XPS results of molybdenum Mo 3d spectrum. The molybdenum metal was fitted by LA(1,1; 2,3; 2) and molybdenum compounds by GL(30). It was detected that in surface layer there were mainly molybdenum compounds in valency states six (65 at%) and five (17,4 at%). The other Mo valency states (2, 3 and 4) as well as metal part of molybdenum spectrum were in the range from 2,4 at% to 5,4 at%.

Table 3 Analyses of Cr 2p spectrum by GL(30) and LA(1.3,4,5) line shapes

BE / eV	573,8	577,0	579,0	573,8	577,0	579,0
FWHM	0,479	2,257	1,921	0,480	2,257	1,921
Line Shape	GL(30)	GL(30)	GL(30)	LA(1,3; 4, 5)	GL(30)	GL(30)
AREA	0,5	40,1	5,4	0,5	40,1	5,4
Cr $2p_{3/2}$ / at%	1,0	87,3	11,7	1,0	87,3	11,7
Oxidation stage	Cr^0	Cr^{3+}	Cr^{6+}	Cr^0	Cr^{3+}	Cr^{6+}
Chromium Compounds	Cr(0)	Cr_2O_3/CrOOH	$(CrO_4)^2$	Cr(0)	Cr_2O_3/CrOOH	$(CrO_4)^2$

Table 4 Analysis of Mo 3D spectrum

Mo $3d_{5/2}$	BE / eV	227,5	228,6	229,8	231,3	232,5	232,9
	FWHM	0,45132	1,2986	0,68264	0,56245	1,36908	1,54734
	Line Shape	LA(1,1; 2,3; 2)	GL(30)	GL(30)	GL(30)	GL(30)	GL(30)
	AREA	0,3	0,3	0,1	0,3	1,1	4,0
	at%	3,24	3,08	1,44	2,8	10,46	38,98
Mo $3d_{3/2}$	BE / eV	230,6	231,8	232,9	234,4	234,5	236,0
	FWHM	0,45132	1,2986	0,68264	0,56245	1,36908	1,54734
	Line Shape	LA(1,1; 2,3; 2)	GL(30)	GL(30)	GL(30)	GL(30)	GL(30)
	AREA	0,2	0,2	0,1	0,2	0,7	2,7
	at%	2,16	2,05	0,96	1,87	6,97	25,99
	Total / at%	5,4	5,1	2,4	4,7	17,4	65,0
		Mo^0	Mo^{2+}	Mo^{3+}	Mo^{4+}	Mo^{5+}	Mo^{6+}

Table 5 2D roughness parameters according to ISO 4287

Ra	0,737	µm	*Ra*: Arithmetic mean deviation of the roughness profile
Rq	0,895	µm	*Rq*: Root-Mean-Square (RMS) Deviation of the roughness profile
Rp	1,72	µm	*Rp*: Maximum peak height of the roughness profile
Rv	1,77	µm	*Rv*: Maximum Valley Depth of the roughness profile
Rt	5,95	µm	*Rt*: Total height of roughness profile
Rz	3,49	µm	*Rz*: Maximum height of roughness profile
Rc	2,26	µm	*Rc*: Mean height of the roughness profile elements
Rsk	0,048	-	*Rsk*: Skewness of the roughness profile
Rku	2,46	-	*Rku*: Kurtosis of the roughness profile

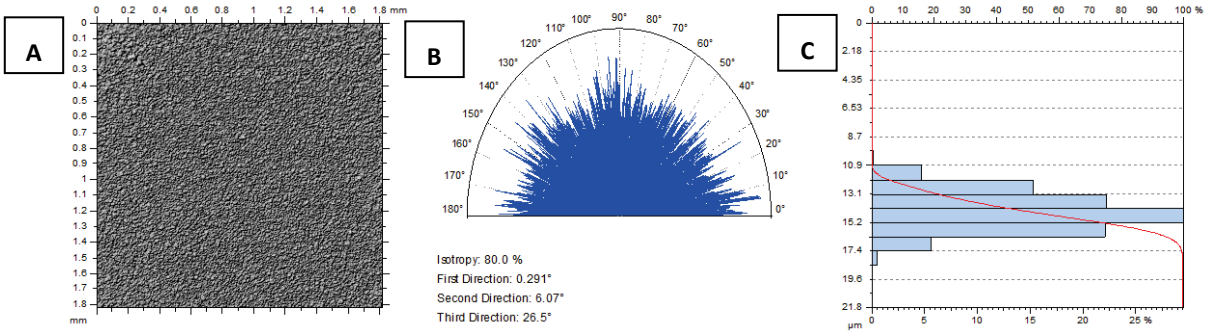

Figure 6 Surface characteristics in 3D: surface simulation (A), texture direction (B), and Abbott-Firestone curve (C)

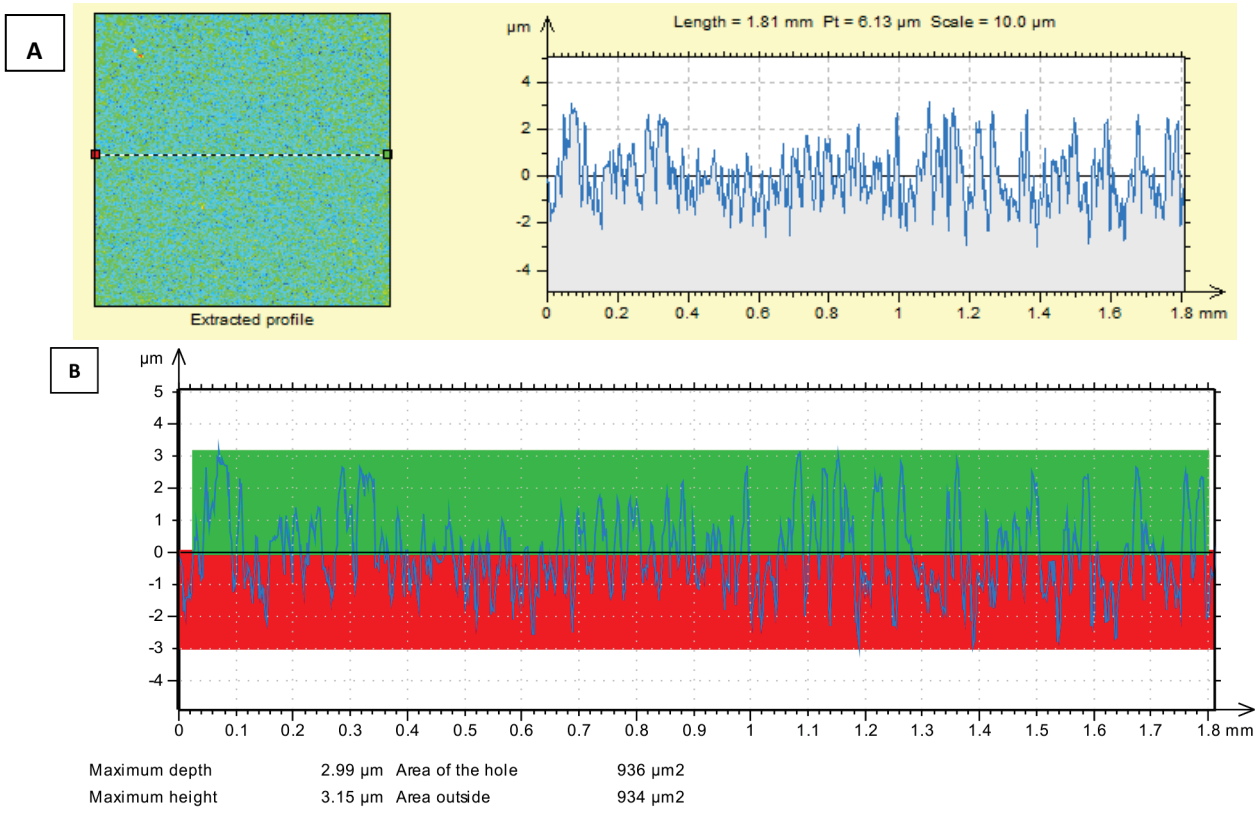

Figure 7 Surface characteristics in 2D: surface simulation (A), roughness profile (B)

Table 6 Height 3D roughness parameters according to ISO 25178

Sa	1,13	µm	*Sa*: Arithmetic mean height
Sq	1,37	µm	*Sq*: Root mean square height
Sp	14,3	µm	*Sp*: Maximum peak height
Sv	7,44	µm	*Sv*: Maximum pit height
Sz	21,8	µm	*Sz*: Maximum height
Ssk	0,253	-	*Ssk*: Skewness
Sku	3,28	-	*Sku*: Kurtosis
Sa	1,13	µm	*Sa*: Arithmetic mean height

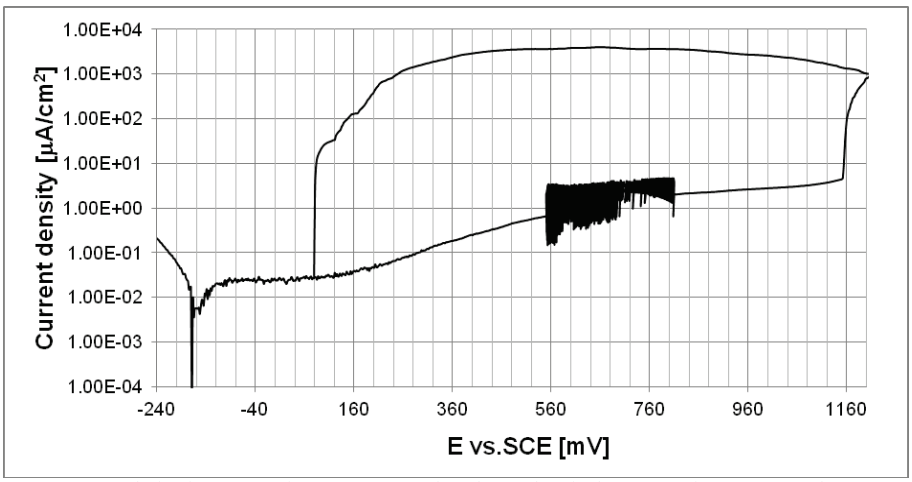

Figure 8 Polarization curve of AISI 316L SS after electrochemical treatment in concentrated HNO_3

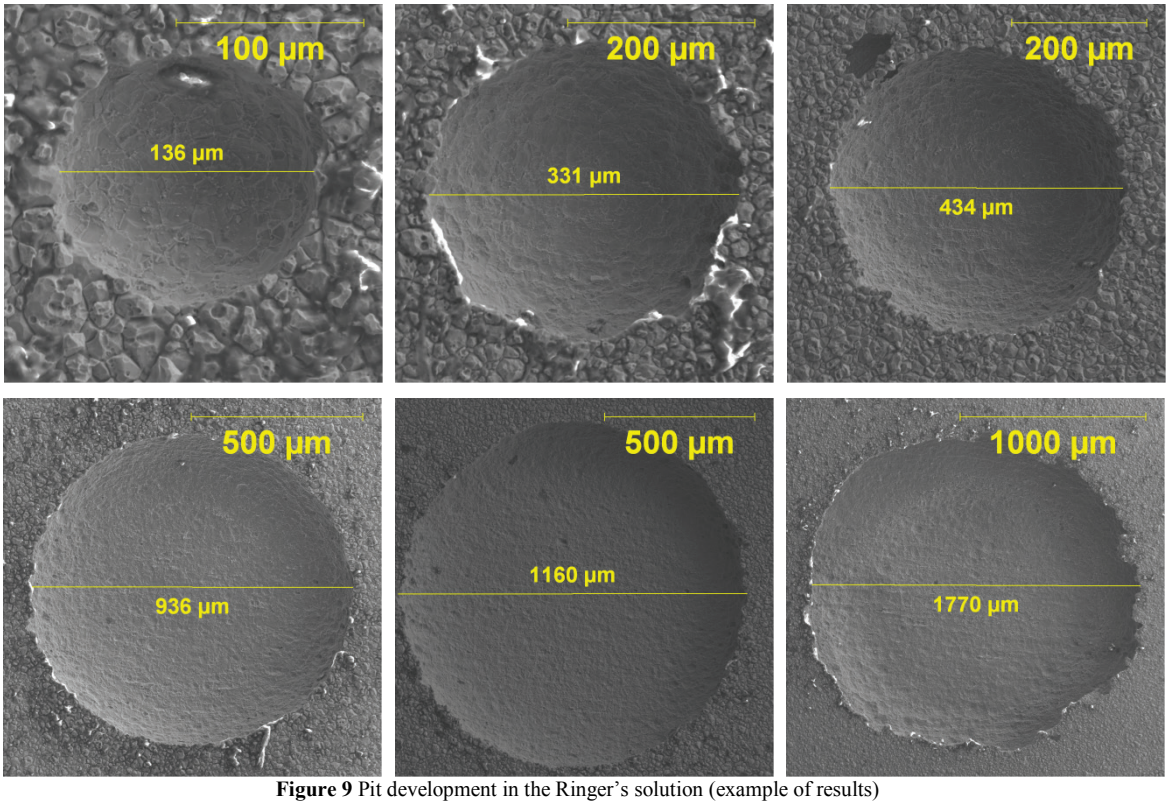

Figure 9 Pit development in the Ringer's solution (example of results)

In Figs. 5 and 6 there are shown the results of surface topography analysis i.e. 3D and 2D surface simulations, texture direction, Abbott-Firestone curve, roughness profile as well as 2D and 3D roughness parameters with Gaussian filter and cut-off equal to 0,08 mm (Tabs. 5 and 6). There is not visible one texture direction what can be observed on the surfaces after mechanical polishing. Obtained surface is uniform, characterized by 2D and 3D roughness parameters: Ra = 0,737 µm, Rq = 0,895 µm and Sa = 1,13 µm, Sq = 1,37 µm.

In Fig. 8 there is shown an exemplary curve of potentiodynamic corrosion measurements of surface after electrochemical treatment in concentrated HNO_3. The average of passive current density equals $2{,}3\times10^{-2}$ µA/cm^2. The pitting corrosion resistance corresponding to pitting potential (1140 mV vs. SCE) is higher than that after a standard electrochemical polishing (E_{pit} = 600 mV vs. SCE), and re-passivation potential equals 79 mV vs. SCE. The dark dense area between 560 mV and 800 mV in Fig. 8 indicates the unstable pits, which undergo to repassivation.

In Fig. 9 there are given SEM photos of pit development in Ringer's solution with the pits of increasing diameters. They were taken on ASPEX EXPLORER™ device from a typical sample after electrochemical corrosion studies.

4 Discussion

In presented paper, there is shown the compact surface film characterization of AISI 316L austenitic stainless steel after electropassivation in HNO_3. It is a novel approach to the subject of surface finishing. The most interesting findings in the article are the analysis of chromium compounds especially of the sixth level oxidation compounds as well as molybdenum states of oxidation on the background of iron compounds analysis. To illustrate the changes after the treatment, the SEM

photos of the sample after proposed electro-passivation with EDX surface analysis (Fig. 1) plus additional information of 3D surface roughness measurements (Figs. 6 and 7, and Tabs. 5 and 6) are given. In order to characterize the corrosion resistance, there were shown the polarization characteristics (Fig. 8), which comprehensively describe the properties of the surface layer formed. The authors' previous results [7, 13] obtained on 316L SS after a standard electropolishing in the Ringer's solution indicate the level of pitting corrosion resistance of about 600 mV versus SCE. In their analysis of AISI 316L surface after electropolishing and passivation in HNO_3 the Henkels [30] show that the difference between the pitting potentials of only electropolished and electropolished plus passivated 316L SS sample was about 100 mV. Other researchers find [21] that nitric acid passivation can increase the pitting potential of AISI 316 stainless steel. Following this reasoning the steel surface after passivation in HNO_3 should be about maximum in the range of (700 ÷ 800) mV vs. SCE. In comparison, the data in this paper show that the pitting potential is equal to 1160 mV only after electro-passivation treatment in HNO_3 (mechanical/ abrasive polishing was used as the pre-treatment only). On the basis of literature data obtained and current knowledge in the field of surface finishing, our results should be considered as much better and the method innovative.

5 Conclusion

In the article there was described the surface obtained after electrochemical treatment in concentrated HNO_3. It was characterized due to roughness, corrosion protection and chemical composition of the surface layer. The obtained roughness was equal to Sa = 1,13 μm (Ra = 0,737 μm), Sq = 1,37 μm (Rq = 0,895 μm). The corrosion resistance in the Ringer's solution was described by a passive current density ($i_{pass} = 2{,}3\times10^{-2}$ μA/cm^2), pitting corrosion potential (E_{pit} = 1140 mV vs. SCE) and re-passivation potential (E_{repass} = 79 mV vs. SCE). The XPS spectroscopy was used to find the composition of the surface layer after the treatment performed. On the basis of obtained data, there were detected the following chemical elements: iron, chromium, molybdenum, cobalt, manganese, as well as calcium (contamination). The high resolution XPS spectra have shown that iron compounds can be described as Fe_2O_3/FeOOH and chromium compounds as Cr_2O_3/CrOOH. Concerning Mo as the alloying element of AISI 316L SS, it was detected that in surface layer there was mainly molybdenum in valency states 6 (65 at%) and 5 (17,4 at%). The Mo valency states such as zero, two, three and four were in the amount range from 2,4 at% to 5,4 at%.

Acknowledgment

Professor Dr Gregor Mori of the Institute of Schadensanalytik, Montanuniversität Leoben, Austria, is greatly acknowledged for getting chemical analysis of the AISI 316L austenitic stainless steel samples. Professor Wojciech Kacalak of the Koszalin University of Technology is acknowledged for making available the instruments of Taylor-Hobson Precision Talysurf CCI 6000. Dr Robert Tomkowski, a specialist of the Laboratory for Micro- and Nanoengineering, is thankful for the surface analysis carried out using the Talysurf CCI 6000.

6 References

[1] Davidson, J. A.; Kovacs, P. Passivation method and passivated implant, Patent EP 0520721 A2 (1992)

[2] Maller, R. R. Passivation of Stainless Steel. // Trends in Food Science and Technology. 9, (1998), pp. 28-32.

[3] Baron, A; Simka, W; Nawrat, G.; Szewieczek, D. Electropolishing and chemical passivation of austenitic steel // J. Achievements in Materials and Manufacturing Engineering. 31, 2(2008), pp. 197-202.

[4] Parsapour, A.; Fathi, M. H.; Salehi, M.; Saatchi, A.; Mehdikhani, M. The Effect of Surface Treatment on Corrosion Behavior of Surgical 316L Stainless Steel Implant. // Intern. J. ISSI. 4, 1-2(2007), pp. 34-38.

[5] http://www.electrohio.com/Finishing/Passivation/Passivation.htm

[6] McCafferty, E. Introduction to Corrosion Science. Springer New York, Dordrecht, Heidelberg, London, DOI: 10.1007/978-1-4419-0455-3 (2010).

[7] Rokosz K. Polerowanie elektrochemiczne stali w polu magnetycznym (Electrochemical polishing of steels in the magnetic field). Monograph Nr 219, Publisher: Koszalin University of Technology, Koszalin 2012, ISSN 0239-7129, (211 pages), (in Polish).

[8] Hryniewicz, T.; Rokicki, R.; Rokosz, K. Magnetoelectropolishing for metal surface modification. // Trans. of the Institute of Metal Finishing. 85, 6(2007), pp. 325-332.

[9] Hryniewicz, T. Concept of microsmoothing in electropolishing process. // Surface and Coatings Technology. 64, 2(1994), pp. 75-80.

[10] Hryniewicz, T.; Rokosz, K. Polarization Characteristics of Magnetoelectropolishing Stainless Steels. // Materials Chemistry and Physics. 122, (2010), pp. 169-174.

[11] Hryniewicz, T.; Rokicki, R.; Rokosz, K. Surface characterization of AISI 316L biomaterials obtained by electropolishing in a magnetic field. // Surface and Coatings Technology. 202, 9(2008), pp. 1668-1673.

[12] Hryniewicz, T.; Rokosz, K.; Rokicki, R. Electrochemical and XPS Studies of AISI 316L Stainless Steel after Electropolishing in a Magnetic Field. // Corrosion Sci. 50, 9(2008), pp. 2676-2681.

[13] Hryniewicz, T.; Rokicki, R.; Rokosz, K. Corrosion Characteristics of Medical Grade AISI 316L Stainless Steel Surface after Electropolishing in a Magnetic Field. // CORROSION (The Journal of Science and Engineering), Corrosion Science Section. 64, 8(2008), pp. 660-665.

[14] Rokicki, R. US Patent No. 7632390 (2009). http://www.patentgenius.com/patent/7632390.html

[15] Product Data Bulletin, 316/316L Stainless Steel, AK Steel Corporation, PD-140 7180-0127 PDF 7/00, (2000). www.aksteel.com

[16] Hryniewicz, T.; Rokosz, K. Investigation of selected surface properties of AISI 316L SS after magnetoelectropolishing. // Materials Chemistry and Physics. 123, (2010), pp. 47-55. DOI: 10.1016/j.matchemphys.2010.03.060

[17] Hloch, S.; Kl'oc, J.; Hreha, P.; Magurová, D.; Kozak, D.; Knapčíková, L. Water jet technology using in orthopaedic surgery. // Tehnicki Vjesnik-Technical Gazette. 20, 2(2013), pp. 351-357.

[18] Rokosz, K.; Hryniewicz, T.; Raaen S. Characterization of Passive Film Formed on AISI 316L Stainless Steel after

Magnetoelectropolishing in a Broad Range of Polarization Parameters.// Steel Research International. 83, 9(2012), pp. 910-918. DOI: 10.1002/srin.201200046
[19] ASTM A967 / A967M - 13 Standard Specification for Chemical Passivation Treatments for Stainless Steel Parts
[20] O'Laoire, C.; Timmins, B.; Kremer, L.; Holmes, J. D.; Morris, M. A. Analysis of the Acid Passivation of Stainless Steel.// Analytical Letters. 39, 11(2006), pp. 2255-2271. DOI: 10.1080/00032710600755363
[21] Noh, J. S.; Laycock, N. J.; Gao, W.; Wells, D. B. Effects of nitric acid passivation on the pitting resistance of 316 stainless steel. // Corrosion Sci. 42, 12(2000), pp. 2069-2084. DOI: 10.1016/S0010-938X(00)00052-4
[22] Fairley, N. http://www.casaxps.com, © Casa software Ltd., (2005).
[23] Walton, J.; Carrick, A. The Casa Cookbook-The CasaXPS User's Manual, Part 1: Recipes for XPS data proceedings. ISBN: 9780954953300, Publisher: Acolyte Science, (2009).
[24] CasaXPS Processing Software, CasaXPS Manual 2.3.15 Rev 1.0, Copyright © 2010 Casa Software Ltd, pp. 19-20.
[25] Herrera-Gomez, A. The Peak-Shirley Background (Shirley background in overlapping peaks). Centro de Investigación y de Estudios Avanzados del IPN Unidad Querétaro, Internal Report Created 8/2011, Last Update 2/2012, (14 pages).
[26] Biesinger, M. C.; Payne, B. P.; Grosvenor, A. P.; Lau, L. W. M.; Gerson, A. R.; Smart, R. St.C. Resolving surface chemical states in XPS analysis of first row transition metals, oxides and hydroxides: Cr, Mn, Fe, Co and Ni. // Applied Surface Science. 257, (2011), pp. 2717-2730.
[27] Rokosz, K.; Hryniewicz, T.; Raaen S. XPS measurements of AISI 430 SS surface after electropolishing operations in a transpassive region of polarisation characteristics. // PAK (Measurement Automation and Monitoring). 58, 1(2012), pp. 126-129.
[28] Rokosz, K.; Hryniewicz, T. XPS measurements of passive film formed on AISI 316l ss after electropolishing in a magnetic field (MEP). // Advances in Materials Science. 34(4) (2012), pp. 13-22. DOI: 10.2478/v10077-012-0012-5
[29] Rokosz, K.; Hryniewicz, T. Cr/Fe Ratio by XPS Spectra of Magnetoelectropolished AISI 316L SS Using Linear, Shirley and Tougaard Methods of Background Subtraction. // Advances in Materials Science. 13, 1(2013), pp. 11-20. DOI: 10.2478/adms-2013-0002
[30] Henkel, G.; Henkel, B. Die passivierung von austenitischen edelstahl- oberflachen in der pharmazeutischen industrie unter berücksichtigung von rougingphänomenen. // Technical Bulletin, HENKEL Beiz- und Elektropoliertechnik GmbH & Co. KG, 2003, www.henkel-epol.com

Authors' addresses

Krzysztof Rokosz
Division of Surface Electrochemistry and Technology
Koszalin University of Technology
Racławicka 15-17,
75-620 Koszalin, Poland
E-mail: rokosz@tu.koszalin.pl

Tadeusz Hryniewicz *(corresponding author)*
Division of Surface Electrochemistry and Technology
Koszalin University of Technology
Racławicka 15-17,
75-620 Koszalin, Poland
E-mail: Tadeusz.Hryniewicz@tu.koszalin.pl

Steinar Raaen
Physics Department
NTNU, NO-7491 Trondheim, Norway
E-mail: sraaen@ntnu.no

Jan Valiček
Institute of Physics, Faculty of Mining and Geology,
VŠB - Technical University of Ostrava,
17. listopadu 15/2172
708 33 Ostrava-Poruba, Czech Republic
E-mail: jan.valicek@vsb.cz